Planar and axial channeling radiation from relativistic electrons in LiF

R. L. Swent, R. H. Pantell, H. Park, J. O. Kephart, and R. K. Klein
Department of Electrical Engineering, Stanford University, Stanford, California 94305

S. Datz and R. W. Fearick*
Oak Ridge National Laboratory, Oak Ridge, Tennessee 37830

B. L. Berman
Lawrence Livermore National Laboratory, University of California, Livermore, California 94550
(Received 1 April 1983; revised manuscript received 11 July 1983)

Channeling radiation has been measured for planar-channeled 16.9-, 30.5-, and ~54.3-MeV electrons and for axial-channeled 16.9-MeV electrons in the ionic crystal LiF. The results are shown to be in reasonable, but not perfect, agreement with calculations which model the crystal as an array of isolated Li^+ and F^- ions.

I. INTRODUCTION AND EXPERIMENT

Radiation from relativistic electrons channeled between crystal planes or along crystal axes has been studied experimentally by several groups (Refs. 1–15). All these experiments have used elemental material (silicon, diamond, germanium, or nickel) for the target crystal. Spontaneous transitions between bound states in the interplanar or interstring potential result in the emission of intense and sharp spectral lines in the forward direction.

We have measured channeling radiation from the compound binary crystal LiF. This material was chosen because of its low average atomic number (Li, $Z=3$, and F, $Z=9$) and high Debye temperature ($\simeq$730 K). These characteristics ensure that the scattering of channeled electrons by thermal vibrations of the crystal atoms will be relatively small. Other factors in the choice were the availability of high-quality samples and the ease of preparation. The 25-μm target used for this experiment was prepared by polishing, followed by etching with water. An x-ray-diffraction measurement of the mosaic spread showed it to be less than the instrumental resolution of 1.5 mrad.

LiF crystals have a rocksalt structure. For such crystals, the planes whose Miller indices are all odd are segregated: Planes consisting entirely of Li atoms alternate with planes of F atoms. Planes with even indices are mixed, and to first order will appear to a channeled electron to be simple planes of atomic number $Z=6$. Similarly, axes whose Miller indices include two and only two odd numbers are segregated; the others are mixed.

The measurements were performed with beams of electrons from the Lawrence Livermore National Laboratory Electron-Positron Linear Accelerator. The experimental apparatus and procedures are described in Ref. 16.

Data were obtained at three incident electron energies: ~54.3, 30.5, and 16.9 MeV. In all cases, the energy spread was $\lesssim$0.25%. The (110) and (111) planes were studied with a 54.2-MeV ($\gamma=107.1$) beam, and a 54.5-MeV ($\gamma=107.6$) beam was used for the (100) plane. For both these and the 30.5-MeV ($\gamma=60.7$) case, the angular divergence of the beam was $\lesssim$0.3 mrad full width at half maximum (FWHM) before striking the crystal. Also used was a 16.9-MeV ($\gamma=34.0$) beam having a divergence of roughly 0.6 mrad FWHM horizontally and 0.4 mrad FWHM vertically. For the high and low beam energies, the photons were measured with a Ge (Li) detector having a resolution of ~2 keV FWHM. The efficiency of this detector is nearly constant for incident photons in the energy region from 30 to 120 keV, and decreases above and below this energy region. This detector viewed the radiation through Al windows of total thickness 0.4 mm. For the intermediate beam energy (30.5 MeV), an intrinsic Ge detector was used, which viewed the radiation through Be windows of total thickness 1.0 mm. This latter detector system thus extends the usable energy range down below 10 keV. Axial-channeling radiation was measured at all three beam energies. Owing to the high density of states at the two higher beam energies, the axial spectra obtained were smooth and featureless; hence only those for the 16.9-MeV electron beam are presented and discussed in this paper.

II. PLANAR-CHANNELING RADIATION

Calculated planar-averaged potentials for electrons channeled along the three major planes in LiF are shown in Figs. 1–3, along with the eigenvalues for the three beam energies listed above. The calculations use the many-beam approximation described in Ref. 5. This approach takes into account the periodicity of the potential, so that the energy levels near the tops of the wells broaden into bands (these bands are shaded in the figures). The Fourier coefficients of the potentials were obtained from the values of the electron-scattering factors $f_e(s)$ for isolated Li^+ and F^- ions given in Ref. 17. The zero-order coefficient was chosen to make the potential nearly zero midway between the planes. For values of the transverse

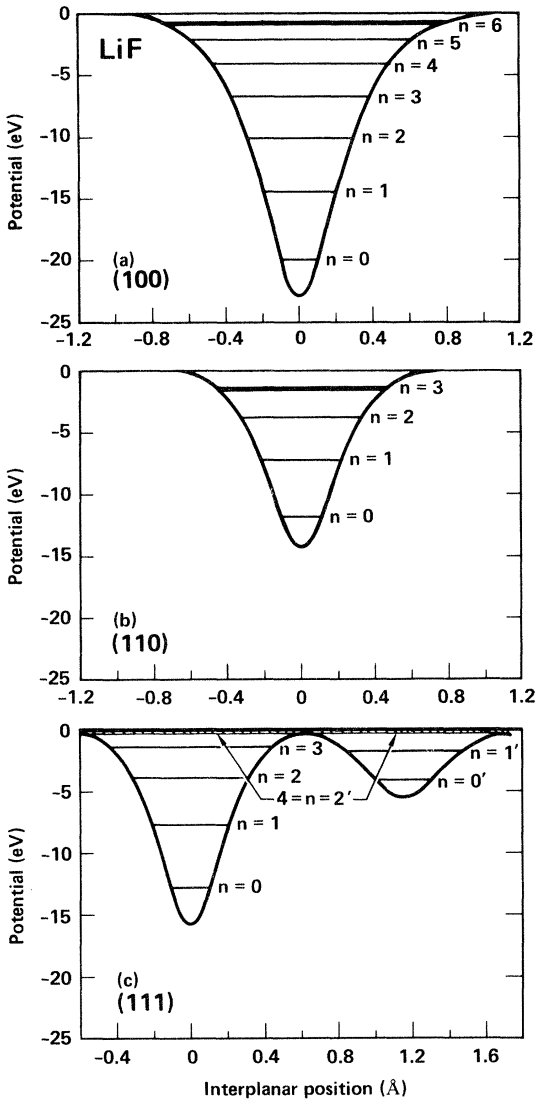

FIG. 1. Calculated interplanar potentials and energy levels [case (a)] for ~54.3-MeV electrons in LiF: (a) for the (100) plane; (b) for the (110) plane; (c) for the (111) plane. In (c), the interplanar position is measured from the fluorine plane; the lithium plane is located at slighly less than 1.2 Å.

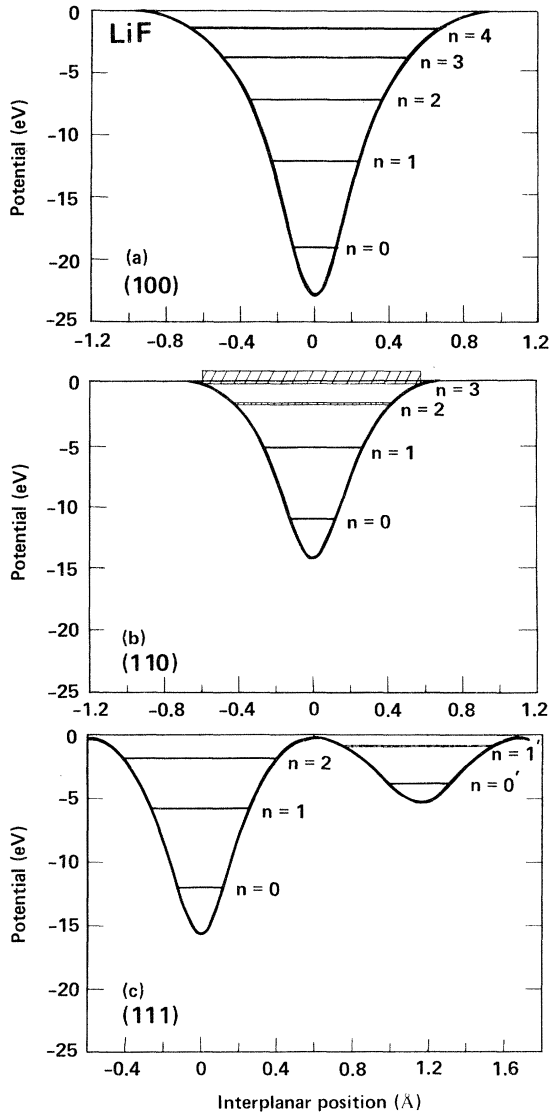

FIG. 2. Calculated interplanar potentials (the same as in Fig. 1) and energy levels [case (a)] for 30.5-MeV electrons in LiF: (a) for the (100) plane; (b) for the (110) plane; (c) for the (111) plane.

wave number s larger than those for which values of $f_e(s)$ were given in Ref. 17, a two-term extrapolation was performed. The first term was a Coulomb term resulting from the ionic charge (which is actually negligible for large s), and the second term was a Lorentzian which was adjusted to give a good fit to the tabulated values of $f_e(s)$. Thermal vibrations were taken into account by multiplying the Fourier coefficients by Debye-Waller factors, using two sets of values for the mean-square vibrational amplitudes. The first set is given in Ref. 18: $\langle U^2 \rangle = 0.0139$ Å^2 for Li and $\langle U^2 \rangle = 0.0085$ Å^2 for F. The second set of calculations used $\langle U^2 \rangle = 0.0139$ Å^2 for Li and $\langle U^2 \rangle = 0.0114$ Å^2 for F. These calculations are referred to below as cases (a) and (b), respectively.

The potentials for the mixed (100) and (110) planes are not qualitatively different from those found in monatomic crystals. The segregated (111) planes, however, have deep F potential wells alternating (with equal spacing) with shallow Li wells. This contrasts with the double-well structure found for the (111) planes in diamond or silicon, where the wells are of equal depth but the spacing is uneven (see Ref. 14).

The measured spectra for these planes are shown in Figs. 4—6. In each case a random spectrum, obtained by aligning the crystal in a nonchanneling direction, has been subtracted. The experimental line energies and widths were extracted by a least-squares procedure which models a spectrum as a series of Lorentzian lines atop a quadratic

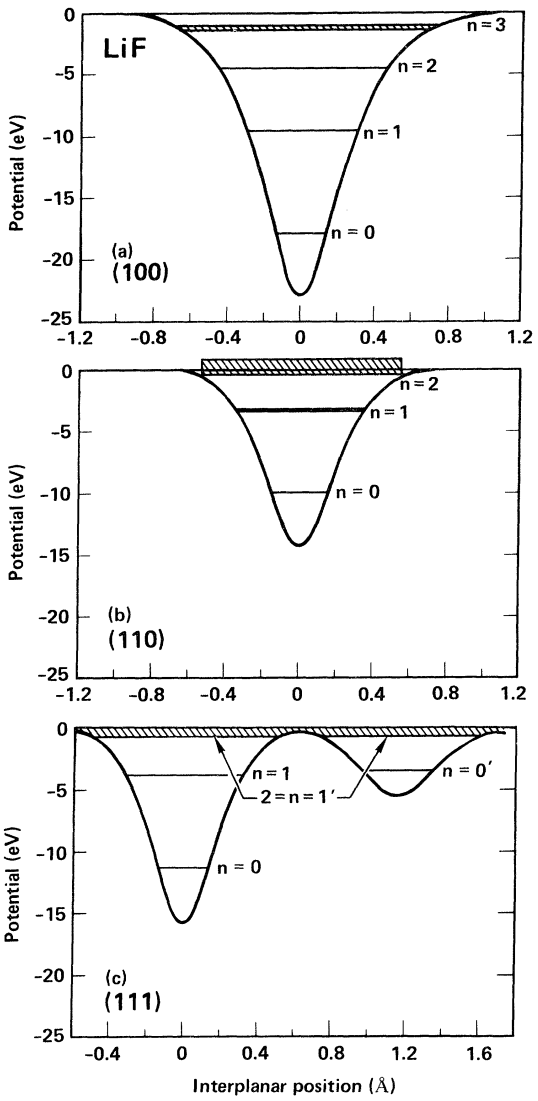

FIG. 3. Calculated interplanar potentials (the same as in Fig. 1) and energy levels [case (a)] for 16.9-MeV electrons in LiF: (a) for the (100) plane; (b) for the (110) plane; (c) for the (111) plane.

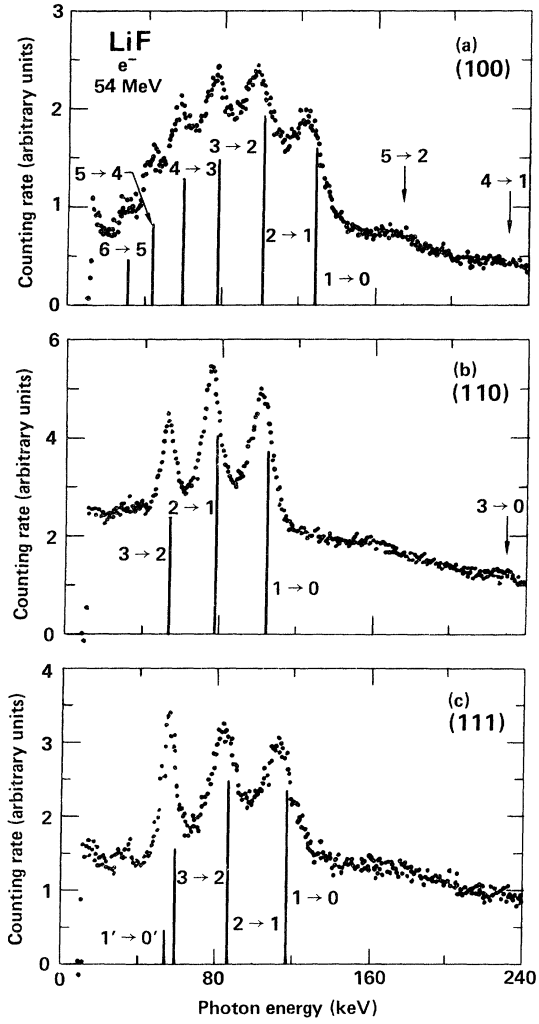

FIG. 4. Measured photon spectra (with random spectra subtracted) for ~54.3-MeV electrons channeled in LiF: (a) along the (100) plane; (b) along the (110) plane; (c) along the (111) plane. The positions of the vertical lines indicate the Doppler-shifted transition energies between the eigenstates of Fig. 1; their heights indicate the relative intensities of these transitions, assuming equal initial level populations.

background. These measured values are given in Table I. A number of $\Delta n = 3$ transitions can be discerned (but only barely) as weak peaks at higher photon energies in the spectra. For a more detailed discussion of $\Delta n = 3$ transitions (for silicon), see Ref. 4.

For the 54-MeV case, the calculated line energies [for case (a)] are very close to the measured values, but are consistently higher. This behavior could result from the use in the calculation of thermal-vibration amplitudes that are too small, particularly because the transitions between states of lower n exhibit the larger disagreements. On the other hand, for the 16.9-MeV case, the calculated line energies [for case (a)] are in general agreement with the measured ones, but are consistently lower.

The channeling of electrons along the (111) planes is unique because of the double-well potential. In the following, the unprimed quantum numbers refer to states localized primarily in the F potential well and the primed numbers to the Li well. Channeling-radiation spectra for 54.2-MeV electrons from this plane are shown in part (c) of Fig. 4 and in Fig. 7. The two highest-energy spectral lines come from the $1 \rightarrow 0$ and $2 \rightarrow 1$ transitions, while the lowest-energy line is a superposition of the $3 \rightarrow 2$ and $1' \rightarrow 0'$ transitions. The $3 \rightarrow 2$ transition is predicted to be about three times as strong as the $1' \rightarrow 0'$ transition, but also about twice as broad. Given equal populations in the $n = 3$ and $n = 1'$ states, the two lines would have roughly equal amplitudes at the peak. For 30.5-MeV electrons, on the other hand [Fig. 5(c)], the lowest-energy line is the $1' \rightarrow 0'$ transition, with very little contribution from any F-well transitions. For 16.9-MeV electrons [Fig. 6(c)], only F-well radiation can be seen because the Li well is too

TABLE I. Comparison of calculated and measured spectral line energies and widths for electrons channeled along planes in LiF.

			Peak energy (keV)			Linewidth FWHM (keV)	
			Calculated			Calculated[a]	
γ	Plane	Transition	(a)	(b)	Measured	(a)	Measured
107.6	(100)	1 →0	128.9	121.4	124.5±1	21.1	22.9±1
		2 →1	101.5	98.1	97.4±1	16.1	23.9±1
		3 →2	78.4	77.2	75.3±1	11.7	17.8±1
		4 →3	59.7	59.4	57.8±1	8.2	14.6±1
		5 →4	44.4	44.5	42.7±2	5.6	b
		6 →5	30—33	30—33	b		b
107.1	(110)	1 →0	105.1	99.3	101.5±1.0	14.3	13.1±0.5
		2 →1	78.2	75.8	75.5±0.8	10.2	10.7±0.4
		3 →2	54.3	53.6	53.2±0.9	7.1	7.2±0.4
107.1	(111)	1 →0	117.1	108.2	112.6±1.0	20.1	19.2±0.5
		2 →1	86.4	82.6	84.1±0.9	14.4	17.0±0.5
		3 →2	59.0	57.9	55.6±0.4	9.2	7.2±0.5
		1′ →0′	54.2	54.0		4.7	
60.7	(100)	1 →0	51.0	48.4	48.8±0.4	6.5	7.3±0.2
		2 →1	36.6	35.9	34.9±0.4	4.5	6.7±0.2
		3 →2	25.5	25.4	24.3±0.4	2.9	4.4±0.2
		4 →3	17.0	17.1	16.1±0.4	2.0	2.5±0.3
60.7	(110)	1 →0	41.3	39.3	38.9±0.4	4.5	4.8±0.1
		2 →1	26.8	26.3	25.3±0.4	3.0	3.5±0.1
60.7	(111)	1 →0	46.0	42.8	43.7±0.4	6.2	6.0±0.2
		2 →1	29.1	28.3	27.8±0.4	3.7	5.0±0.2
		1′ →0′	20.7	20.6	20.6±0.4	1.9	2.0±0.2
34.0	(100)	1 →0	19.5	18.7	20.0±0.7	2.9	3.9±0.5
34.0	(110)	1 →0	15.4	14.8	15.8±0.7	2.5	2.9±0.5
34.0	(111)	1 →0	17.0	16.1	17.5±0.7	2.7	2.9±0.5

[a]The linewidths calculated for case (b) are only slightly larger than those for case (a).
[b]Not well determined from the data [see Fig. 4(a)].

shallow to support more than a single bound state.

Figure 7 shows the (111) channeling-radiation spectra for 54.2-MeV electrons (with random spectra subtracted) for several angles of incidence of the electron beam. The results of least-squares fits to the spectra are shown, assuming three Lorentzian lines and a baseline (also shown) described by a second-order polynomial. The variation of the incidence angle was accomplished by tilting the crystal while the beam and the detector were held fixed. Thus, for a given incidence angle ϕ, the observation angle (relative to the crystal planes) is equal to the same angle ϕ. As a consequence of the Doppler shift, the photon energies decrease with increasing incidence angle. The intensities of the lines also decrease as the incidence angle increases, and the interesting feature is that the lowest-energy line decreases in intensity faster than do the other two lines.

The reduction of the intensity is caused primarily by the change in the initial distribution of population. As the incidence angle increases, so does the transverse energy of the beam, and electrons will be captured preferentially into states with higher transverse energy. On the basis of this effect, one would expect the intensity of the low-n transitions to decrease relative to those of the high-n transitions as the incidence angle increases. The observed behavior is just the opposite. Figure 8 shows the normalized line intensities versus incidence angle. It is clear that the intensities are affected not only by the initial conditions, but also by the subsequent redistribution of the bound-state populations.

In the case of a simple plane (i.e., one with a single-well potential), it is believed that incoherent scattering causes the bound-state populations to become equal within a short distance (~ 4 μm for 54-MeV electrons in Si), and the populations decay slowly with further penetration. In the present case, there are two sets of bound states (primed and unprimed) which are only weakly coupled to each other, but both sets are coupled to the free states which lie above both (see Fig. 1). Thus the population dynamics, which determines the line intensities, is expected to be considerably more complicated in this case. As a result, studies of channeling along the (111) planes in LiF may constitute the best test for theories which attempt to explain the population dynamics of planar-channeled electrons.

Calculated linewidths also are listed in Table I (the details of these calculations are given in Ref. 19). The calculated width is the sum, in quadrature, of the widths from four sources: (1) thermal incoherent scattering, which limits the lifetime of the states; (2) Doppler shifts, resulting from the angular spread of the electron beam caused by

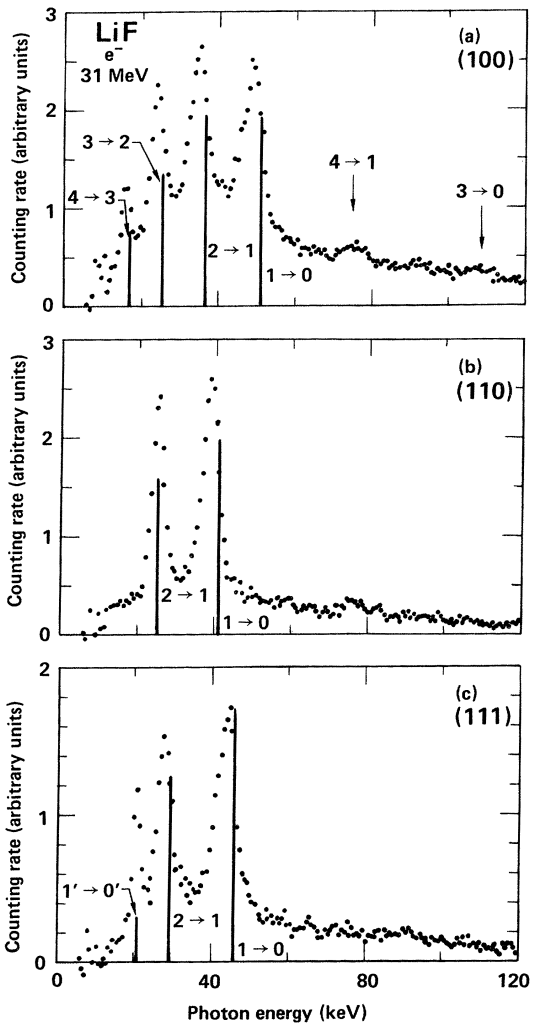

FIG. 5. Measured photon spectra (with random spectra subtracted) for 30.5-MeV electrons channeled in LiF: (a) along the (100) plane; (b) along the (110) plane; (c) along the (111) plane. The positions of the vertical lines indicate the Doppler-shifted transition energies between the eigenstates of Fig. 2; their heights indicate the relative intensities of these transitions, assuming equal initial level populations.

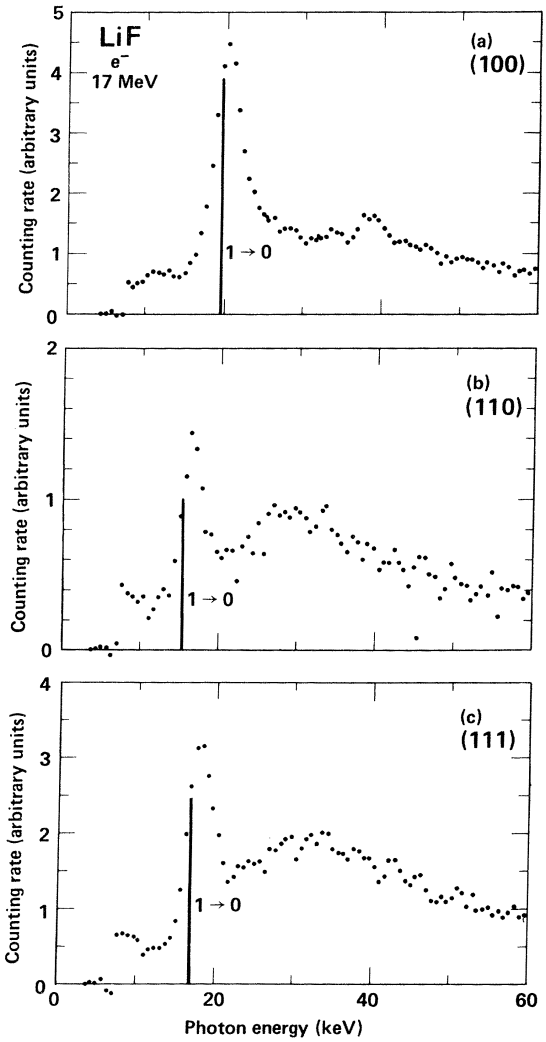

FIG. 6. Measured photon spectra (with random spectra subtracted) for 16.9-MeV electrons channeled in LiF: (a) along the (100) plane; (b) along the (110) plane; (c) along the (111) plane. The positions of the vertical lines indicate the Doppler-shifted transition energies between the eigenstates of Fig. 3; their heights indicate the relative intensities of these transitions, assuming equal initial level populations.

multiple scattering in the crystal; (3) energy-band curvature, which gives a range of energies for a given $i \rightarrow f$ transition; and (4) detector resolution, which is important only for the case of $\gamma = 34$. Except for those for the (100) plane, the calculated widths are reasonably close to the measured values. The data from the (100) plane are unusual in that the linewidths not only are considerably larger than the calculated values, but also are much larger than those for the corresponding transitions in the other planes. Also, at 54 MeV, the $2 \rightarrow 1$ width appears to be at least as large as the $1 \rightarrow 0$ width. The latter fact violates the trend seen for other planes and with other materials; the $1 \rightarrow 0$ transition is usually the broadest because the ground state has a larger overlap with the vibrating atoms than do the higher-lying states.

Turning again to the transition energies, we see that the result of calculation (a) for the (111) plane for 30.5-MeV electrons agrees very well with the measurement for the $1' \rightarrow 0'$ (the Li-well) transition at 20.6 keV, but gives results that are significantly too high for the F-well transitions. This suggests that the value for the fluorine thermal-vibration amplitude given in Ref. 18 is too low. Accordingly, we repeated the calculations using a larger value for F, namely, $\langle U^2 \rangle = 0.0114$ Å^2. The results of these calculations are listed in the column labeled (b) in Table I. Although these calculations yield somewhat better predictions for the $1 \rightarrow 0$ transitions for 30.5- and 54-MeV electrons, the calculated values of the higher-n transition energies are still too high. In addition, these calculations seriously underestimate the $1 \rightarrow 0$ transition energies for 16.9-MeV electrons.

For the two higher beam energies, the $n = 0$ and $n = 1$

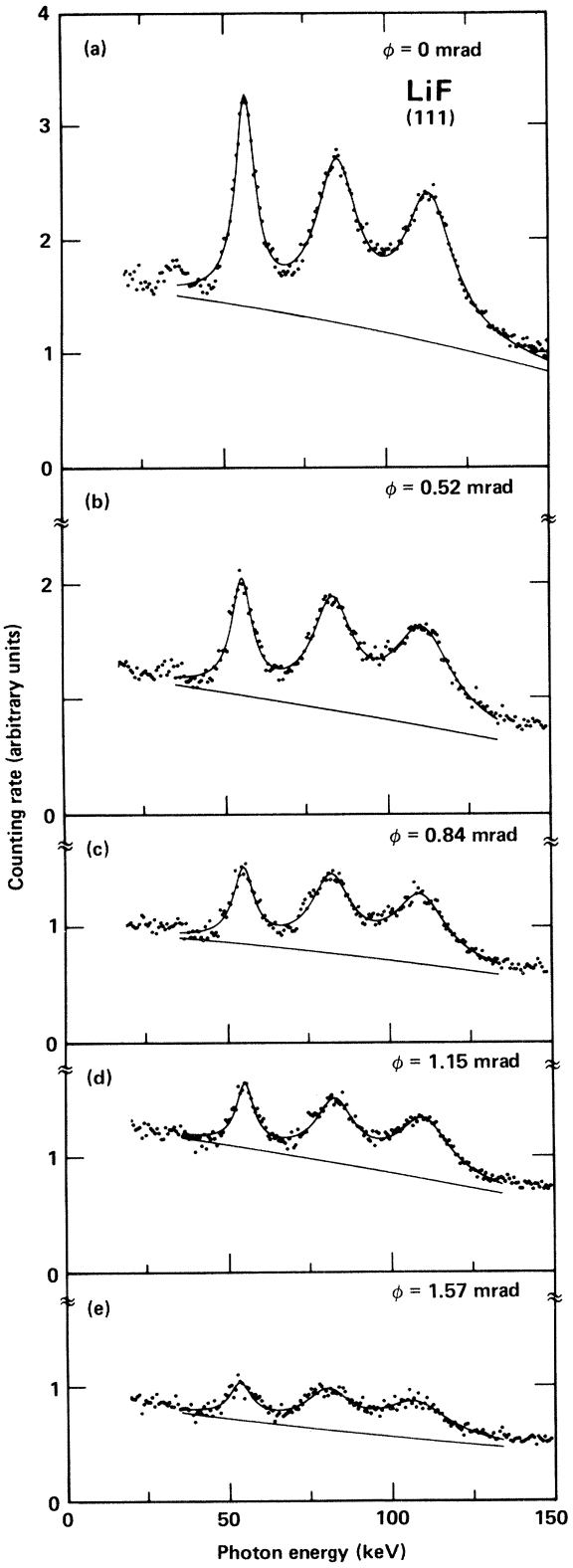

FIG. 7. Measured photon spectra (with random spectra subtracted) for 54.2-MeV electrons channeled along the (111) planes in LiF, for various values of the incidence angle ϕ [the top spectrum (for $\phi=0$) is the one in Fig. 4(c)]. The curves are Lorentz-line fits to the three major peaks atop a baseline (also shown) which is parametrized by a second-order polynomial.

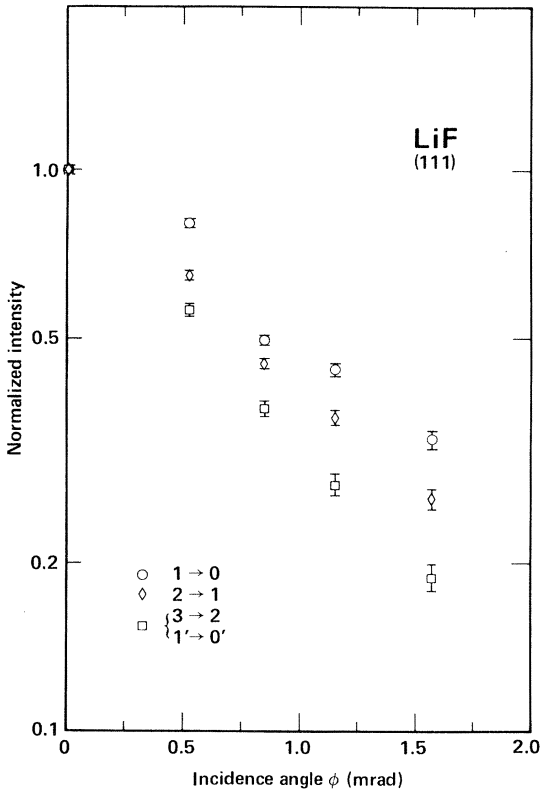

FIG. 8. Normalized intensities (peak height times linewidth) of the three major lines in the (111) spectra shown in Fig. 7, plotted as a function of the incidence angle. The circles indicate the $1\rightarrow0$ line, the diamonds indicate the $2\rightarrow1$ line, and the squares indicate the (unresolved) $3\rightarrow2$ and $1'\rightarrow0'$ doublet.

states are localized near the minima of the potentials (i.e., near the atomic planes), and therefore the energies of the $1\rightarrow0$ transitions are very sensitive to the thermal-vibration amplitudes. For 16.9-MeV electrons, however, these states are more spread out, and therefore are sensitive to the potential farther away from the centers of the planes. Thus, although increasing the fluorine thermal-vibration amplitude seems to improve our potential model near the minima, it appears that this simple model is still inadequate at somewhat larger distances ($\sim$0.2–0.7 Å) from the atoms. Since our calculated energies for the high-n transitions are consistently too high, the model potential apparently is deeper and varies more rapidly with interplanar distance than the actual crystalline potential.

The scaling of the transition energies with incident beam energy is of considerable interest.[1,20] For a (one-dimensional) potential whose dependence upon the coordinate is a simple power law, the transition energies will scale as a power of the beam energy. That is, if $V(x)=ax^m$, then the observed photon energy will vary as $\hbar\omega=b\gamma^\alpha$. For such a potential, the Schrödinger equation in the rest frame (an inertial frame of reference moving at the longitudinal beam velocity) can be put into a form that depends explicitly upon γ only in the eigenvalue term. In this case, the eigenvalues are seen to be proportional to

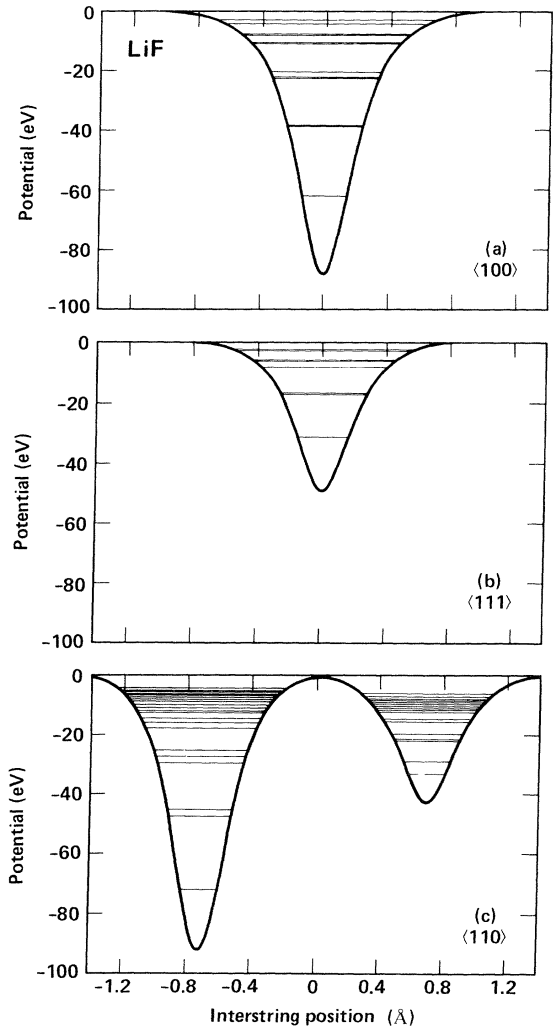

FIG. 9. Calculated axial potentials and energy levels for 16.9-MeV electrons in LiF: (a) for the ⟨100⟩ axis, plotted along the (001) direction; (b) for the ⟨111⟩ axis, plotted along the (112) direction; (c) for the ⟨110⟩ axis. In (c), the interstring position is measured from a point midway between the fluorine string (left) and the lithium string (right), located at $\sim\pm 0.7$ Å. For all three cases, we can identify the lowest, isolated level with the 1*s* level; the next higher-lying doublet with the 2*p* levels; and the next higher-lying triplet with the 2*s* and 3*d* levels.

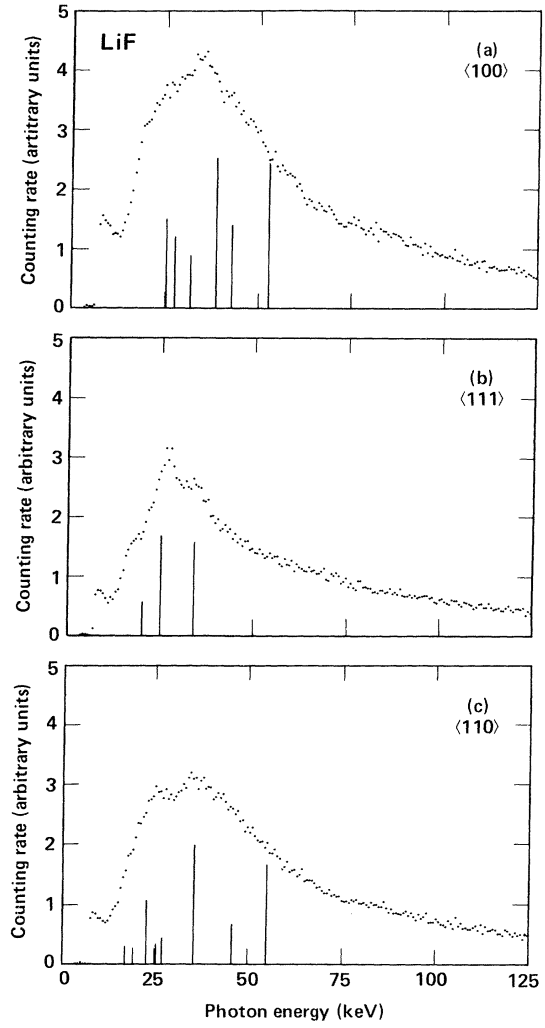

FIG. 10. Measured photon spectra (with random spectra subtracted) for 16.9-MeV electrons channeled in LiF: (a) along the ⟨100⟩ axis, (b) along the ⟨111⟩ axis; (c) along the ⟨110⟩ axis. The positions of the vertical lines indicate the Doppler-shifted transition energies between the eigenstates of Fig. 9; their heights indicate the relative intensities of these transitions, assuming equal initial level populations. A partial identification of the transitions is given in the text.

$\gamma^{2/(m+2)}$. Multiplying this by 2γ to obtain the photon energy as observed in the laboratory frame, we find that the photon energy obeys the relation $\hbar\omega = b\gamma^{1+[2/(m+2)]}$, i.e., $\alpha = 1+[2/(m+2)]$.

It can be seen in Fig. 1(a) that one can describe the interplanar potential for electrons in the following qualitative manner (excluding the region with $|x| \lesssim 0.1$ Å): the potential is linear in x for small x and approaches a constant at larger values. In other words, m is 1 for small values of x and approaches 0 for larger values. On this basis, we expect low-n transitions to exhibit a value of α close to $\frac{5}{3}$, whereas the value of α for high-n transitions should approach 2.

Values of the scaling parameter α can be extracted from our data by taking the electron energies in pairs. The values of α obtained this way are given in Table II. The trends are just as expected, based upon the argument given above. The $4\rightarrow 3$ transition in the (100) plane gives a value of α which is greater than 2. This arises because the crystal potential is periodic. A state with an energy level near the top of the well not only is broadened but also can be shifted (on the average) by the proximity of the neighboring wells. The decrease of the potential at distances greater than half of the interplanar spacing corresponds to a negative value of m, resulting in $\alpha > 2$. It also is very interesting that the low-energy spectral line corresponding

TABLE II. Scaling parameter α for the transition energies.

Plane	Transition	Electron energy range[a] Low-medium	Medium-high	Low-high
(100)	$1 \rightarrow 0$	1.54	1.64	1.59
	$2 \rightarrow 1$		1.79	
	$3 \rightarrow 2$		1.98	
	$4 \rightarrow 3$		2.23	
(110)	$1 \rightarrow 0$	1.56	1.64	1.59
	$2 \rightarrow 1$		1.93	
(111)	$1 \rightarrow 0$	1.58	1.67	1.62
	$2 \rightarrow 1$		1.95	
	$3 \rightarrow 2$		1.75	
	$1' \rightarrow 0'$			

[a]Low: $\gamma = 34.0$ (Fig. 6); medium: $\gamma = 60.7$ (Fig. 5); high: $\gamma = 107.6$ for (100), 107.1 for (110) and (111) (Fig. 4).

to the $1' \rightarrow 0'$ transition for the (111) plane scales like a low-n transition, which in fact it is.

III. AXIAL-CHANNELING RADIATION

For axial-channeling radiation, the situation is more complex. Low beam energies are required if one is to see distinct lines in an axial-channeling spectrum because there are more bound states in an axial (two-dimensional) potential than in a planar potential at the same beam energy. A simple phase-space estimate of the number of bound states for axially channeled electrons is[21] $n = (\gamma Z)/(\pi^3 N d^2 a_0)$, where Z is the atomic number of the crystal atoms, N is the number of atoms per unit volume, d is the spacing of atoms along the axis, and a_0 is the Bohr radius. Using $\gamma = 34$ and an average Z of 6, the resulting estimates are 25 bound states for the $\langle 100 \rangle$ axis and 8 for the $\langle 111 \rangle$ axis. The $\langle 110 \rangle$ axis contains separate Li and F strings, and the estimates are 19 states for the F strings and 6 for the Li strings. These numbers all are fairly large, so that an absence of distinct lines is not unexpected.

However, although complicated, it is still possible to perform a many-beam calculation to attempt to determine the axial energy levels and anticipated line energies. We have performed such calculations, with 11×11 (121-beam) and 15×15 (225-beam) many-beam programs. The Fourier coefficients were obtained from the electron-scattering factors $f_e(s)$ for isolated neutral atoms given in Ref. 17. The thermal vibrations were taken into account by the Debye-Waller factor, using a two-dimensional root-mean-square vibrational amplitude of 0.141 Å for both Li and F atoms. The resulting axially-averaged potentials, along with the calculated energy levels for $\gamma = 34$, are shown in Fig. 9. One sees that the above simple estimate of the number of levels is only roughly correct (there are 12 bound states for the $\langle 100 \rangle$ axis [Fig. 9(a)], 8 for the $\langle 111 \rangle$ axis [Fig. 9(b)], and 21 and 17 for the F and Li strings, respectively, for the $\langle 110 \rangle$ axis [Fig. 9(c)]). More important, however, partly because of occasional degeneracies and partly because some transitions are very weak, we expect, in effect, only six strong lines for the $\langle 100 \rangle$ axis, three for the $\langle 111 \rangle$ axis, and eight for the $\langle 110 \rangle$ axis.

The measured axial spectra for 16.9-MeV electrons channeled along the three major axes are shown (with random spectra subtracted), together with the calculated line energies and strengths, in Fig. 10. It can be seen from this figure that the calculated line energies and strengths correspond remarkably well to the observed channeling-radiation strength distributions. The calculated results for the $\langle 111 \rangle$ axis in particular [Fig. 10(b)], perhaps because this is the simplest case [Fig. 9(b)], are seen to be in detailed agreement with the data, with respect to both strength and structure. In fact, for this case at least, we can identify the transitions in this two-dimensional potential with the spectral lines: The two $2p \rightarrow 1s$ transitions with the line that is highest in energy (at 33.7 keV); the four $3d \rightarrow 2p$ transitions with the next (at 25.3 keV); and the two $2s \rightarrow 2p$ transitions with the third (at 20.4 keV). There even is (weak) evidence for the $3p \rightarrow 1s$ transitions at ~ 68 keV.

IV. SUMMARY

Radiation from electrons channeled in LiF has been measured for electron energies of 16.9, 30.5, and ~ 54.3 MeV. The results of simple calculations are in moderate agreement with the planar-channeling data, but there are some systematic discrepancies which cannot be explained by merely changing the thermal-vibration amplitude. The calculated results for axial-channeling radiation agree with the 16.9-MeV data; but a lower beam energy is required to resolve the spectral lines clearly.

ACKNOWLEDGMENTS

The authors wish to thank Dr. E. Laegsgaard for a very valuable discussion. This work was performed at Lawrence Livermore National Laboratory under the auspices of the U.S. Department of Energy under Contract No. W-7405-eng-48, and was supported in part by the U.S. Air Force Office of Scientific Research under Grant No. AFOSR-81-0209, by the U.S. Joint Services

Electronics Program, under Grant No. DAAG-29-81-K-0057, and by the National Science Foundation under Grant No. ECS-18139. Two of us (S.D. and R.W.F.) acknowledge the support of the Office of Basic Energy Sciences, U.S. Department of Energy, under Contract No. W-7405-eng-26 with Union Carbide Corporation; one of us (R.W.F.) also acknowledges the support of the Council for Scientific and Industrial Research of South Africa.

---

*Permanent address: University of the Witwatersrand, Johannesburg 2001, South Africa.

[1]R. L. Swent, R. H. Pantell, M. J. Alguard, B. L. Berman, S. D. Bloom, and S. Datz, Phys. Rev. Lett. 43, 1723 (1979).

[2]J. U. Andersen and E. Laegsgaard, Phys. Rev. Lett. 44, 1079 (1980).

[3]N. Cue, E. Bonderup, B. B. Marsh, H. Bakhru, R. E. Benenson, R. Haight, K. Inglis, and G. O. Williams, Phys. Lett. 80A, 26 (1980).

[4]B. L. Berman, S. D. Bloom, S. Datz, M. J. Alguard, R. L. Swent, and R. H. Pantell, Phys. Lett. 82A, 459 (1981).

[5]J. U. Andersen, K. R. Eriksen, and E. Laegsgaard, Physica Scr. 24, 588 (1981).

[6]J. E. Watson and J. S. Koehler, Phys. Rev. A 24, 861 (1981).

[7]M. Gouanère, D. Sillou, M. Spighel, N. Cue, M. J. Gaillard, R. G. Kirsch, J.-C. Poizat, J. Remillieux, B. L. Berman, P. Catillon, L. Roussel, and G. M. Temmer, Nucl. Instrum. Methods 194, 225 (1982).

[8]J. U. Andersen, E. Bonderup, E. Laegsgaard, B. B. Marsh, and A. H. Sørensen, Nucl. Instrum. Methods 194, 209 (1982).

[9]J. U. Andersen, S. Datz, E. Laegsgaard, J. P. F. Sellschop, and A. H. Sørensen, Phys. Rev. Lett. 49, 215 (1982).

[10]J. E. Watson and J. Koehler, Phys. Rev. B 25, 3079 (1982).

[11]M. Atkinson, *et al.*, Phys. Lett. 110B, 162 (1982).

[12]V. B. Ganenko, I. I. Miroshnichenko, E. V. Pegushin, V. M. Sanin, and S. V. Shalatskij, Radiat. Effects 62, 167 (1982).

[13]H. Park, R. L. Swent, J. O. Kephart, R. H. Pantell, B. L. Berman, S. Datz, and R. W. Fearick, Phys. Lett. 96A, 45 (1983).

[14]S. Datz, R. W. Fearick, H. Park, R. H. Pantell, R. L. Swent, J. O. Kephart, R. K. Klein, and B. L. Berman, Phys. Lett. 96A, 314 (1983).

[15]J. U. Andersen, E. Bonderup, E. Laegsgaard, and A. H. Sørensen (unpublished).

[16]M. J. Alguard, R. L. Swent, R. H. Pantell, B. L. Berman, S. D. Bloom, and S. Datz, IEEE Trans. Nucl. Sci. NS-26, 3865 (1979); B. L. Berman and S. D. Bloom, Energy Tech. Rev. 81-1, 1 (1981); B. L. Berman, S. Datz, R. W. Fearick, J. O. Kephart, R. H. Pantell, H. Park, and R. L. Swent, Phys. Rev. Lett. 49, 474 (1982).

[17]*International Tables for X-Ray Crystallography,* edited by N. F. M. Henry and K. Lonsdale (Kynoch, Birmingham, England, 1959), Vol. II, p. 164.

[18]H. Witte and E. Wölfel, Rev. Mod. Phys. 30, 51 (1958).

[19]R. L. Swent, Ph.D. thesis, Stanford University, 1982 (unpublished).

[20]M. J. Alguard, R. L. Swent, R. H. Pantell, B. L. Berman, S. D. Bloom, and S. Datz, Phys. Rev. Lett. 42, 1148 (1979).

[21]D. S. Gemmel, Rev. Mod. Phys. 46, 129 (1974).